Article

Potential of Branched Polymers in the Field of Gas Absorption: Experimental Gas Solubilities and Modeling

Jrn Rolker, Matthias Seiler, Liudmila Mokrushina, and Wolfgang Arlt

Ind. Eng. Chem. Res., **2007**, 46 (20), 6572-6583 • DOI: 10.1021/ie061637f

Potential of Branched Polymers in the Field of Gas Absorption: Experimental Gas Solubilities and Modeling

Jörn Rolker,[†] Matthias Seiler,[‡] Liudmila Mokrushina,[†] and Wolfgang Arlt*,[†]

Separation Science & Technology, Friedrich-Alexander-University of Erlangen-Nuremberg, Egerlandstrasse 3, D-91058 Erlangen, Germany, and Process Technology & Engineering, VT-F, Degussa GmbH, Rodenbacher Chaussee 4, D-63457 Hanau, Germany

In this work, the potential of low-viscous branched polymers for gas separation applications such as CO_2 absorption from flue gas is examined. Carbon dioxide and nitrogen solubilities are measured at low pressures for linear and branched polyethers, hyperbranched polyesters, and polyamines such as a polyamidoamine and a polyethylene imine as well as in their aqueous solutions. The results are reported in terms of Henry constants in the temperature range $T = 310-370$ K. The densities of the pure polymers and their aqueous solutions are measured between $T = 293.15$ and 363.15 K. The selectivities of the polymers for CO_2/N_2 and the enthalpies of absorption at infinite dilution are determined. The group-contribution method UNIFAC-FV is applied to the CO_2 solubilities in polyethers and the hyperbranched polyester. It has been shown that branched polymers are promising candidates for gas absorbents with a high capacity for CO_2 and with large selectivities. The UNIFAC-FV model is able to predict the CO_2 solubilities in the investigated polymers.

1. Introduction

Recently, hyperbranched polymers have been suggested as an interesting new "optimization tool" for various separation processes such as extractive distillation, membrane processes, extraction, and adsorption.[1,2] All mentioned applications benefit from the "molecular" features offered by hyperbranched polymers and might lead to less cost-intensive operation. A large number of reviews focus on the characterization of the properties that make hyperbranched polymers special and interesting in the field of chemical engineering; hence only a brief characterization is given here.[1−6]

Hyperbranched polymers are highly branched polydisperse macromolecules with a treelike topology and a large number of functional groups. Important physical properties such as the glass transition temperature of the amorphous components and the solubility behavior are determined from the structure and the type of functional groups. At room temperature, many branched polymers are liquids above their glass temperatures and exhibit low viscosities in the pure state as well as in solution due to the absence of chain entanglement. Furthermore, they are obtained from one-pot syntheses and are available on a large scale at low costs (≥4 EUR/kg). It is possible to "tailor" desired properties for specified industrial tasks and needs by modification of the functional groups or structural variations. Along with monodisperse dendrimers, the hyperbranched polymers are referred to as dendritic polymers. The dendrimers differ because of their perfectly generated symmetrical structure but are only accessible by time-consuming multistep syntheses and therefore are not considered for large-scale applications. Since dendrimers offer a unique structural perfection, they exhibit unique physical properties, but for many applications hyperbranched polymers are sufficient because they can be synthesized with similar physical properties.

As pointed out by several researchers, hyperbranched polymers show a remarkable selectivity and capacity for different processes such as extraction or as an immobilized liquid membrane.[7,8]

In this article we introduce branched polymers to gas absorption, namely flue gas applications (coal-fired or gas-fired power plants) that demand basically a CO_2/N_2 separation in the scope of slowing down climate change, and discuss their potential. So far, we have focused on branched polymers that are commercially available. We consider this study as a first step, followed by stronger efforts on the "tailor-made" path, to optimize branched polymers in terms of capacity, selectivity, and stability with regard to economic demands. In addition to the thermodynamic experiments, kinetic investigations on the CO_2 absorption behavior in promising branched polymers are still to be done. The kinetics also play an important role in absorption but are not discussed in this work.

Concerning the global warming effect which is attributed by many researchers to the increase of the environmental CO_2 concentration, large efforts have been made to find the most economical way for CO_2 sequestration (capture and storage).[9−11] Gas-fired and especially coal-fired power plants are some of the largest emission sources of carbon dioxide. At present, CO_2 scrubbing with aqueous 30 wt % monoethanolamine (MEA) solutions is the state-of-the-art chemical absorption process, accepting several disadvantages:

(a) Solvent regeneration at high temperatures (up to 413 K) causes around 10% decrease in power generation efficiency (LHV basis) if the absorption process is integrated in the power plant.[10]

(b) Another disadvantage are solvent losses due to finite vapor pressure of the solvent (0.5−2 kg of MEA/ton of CO_2 captured).[11]

(c) Deactivation of the solvent by formation of heat-stable salts with oxygen (energy-intensive reclaiming is necessary) and corrosion in the plant are a third disadvantage.

Chemical absorption seems to be still advantageous because of the very low thermodynamic driving forces from the flue gas into the absorbent. The CO_2 concentration in the flue gas may vary between 3 and 12 mol %. Moreover, the process is carried out at ambient pressure, so partial pressures of 0.03−

* To whom correspondence should be addressed. Tel.: +49 9131 85 27440. Fax: +49 9131 85 27441. E-mail: wolfgang.arlt@cbi.uni-erlangen.de.

[†] Friedrich-Alexander-University of Erlangen-Nuremberg.

[‡] Degussa GmbH.

10.1021/ie061637f CCC: $37.00
Published on Web 08/28/2007

Table 1. Characteristics of Utilized Polymer Samples[a]

sample	molar mass [g/mol]	M_w/M_n	functionality/number of functionalities	viscosity (at 298.15 K) [mPa s]	provider	further details
Polyether 1 (branched polyether)	$M_n = 2187$	1.26	OH/6	n.a.[b]	Degussa AG	
Polyether 2 (linear polyether)	$M_n = 501$	1.09	OH/1	60	Degussa AG	
Polyether 3 (linear polyether)	$M_n = 561$	1.09	CH_3/1	37	Degussa AG	
B-U3000 (hyperbranched polyester)	$M_n = 6500$	1.5	OH/2, C_{16-18}-alkanes/14	1500	Perstorp	for Boltorn series: Mackay and Carmezini[27]
B-H2004 (hyperbranched polyester)	$M_w = 3200$		OH/6, medium alkanes/10	15000	Perstorp	
PAMAM (dendrimer polyamindoamine)	$M_n = 3130$	<1.04	OH/16	n.a.[b]	Dendritech	Frechet[6]
Lupasol FG (hyperbranched polyethylene imine)	$M_n = 615$	1.3	NH_2/n.a.[b]	8000	BASF	Petersen[12]

[a] All data were provided by the suppliers. [b] Not available.

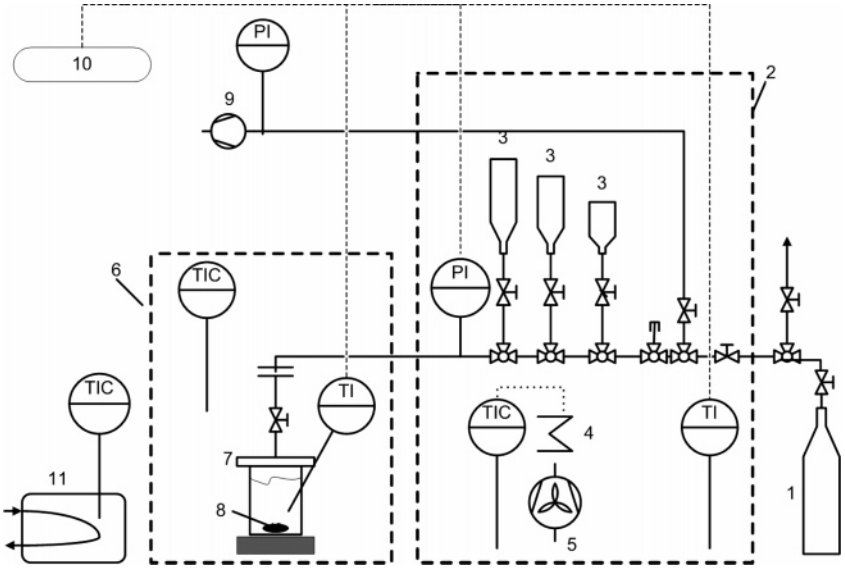

Figure 1. Schematic diagram of the gas solubility apparatus: (1) gas reservoir; (2) air thermostat; (3) gas system; (4) electrical heating; (5) fan; (6) air thermostat; (7) measuring cell; (8) magnetic stirrer; (9) vacuum pump; (10) multimeter and PC; (11) vibrating U-tube densimeter.

0.12 bar are predominant at low temperatures of about 313 K. In total, this situation is challenging.

Facing the drawbacks of conventional amine systems, it is our intention to start an optimization of the CO_2 removal process with the choice of the proper solvent to achieve a physical absorption (leading to the reduction of the energy requirement for regeneration) with a high selectivity and capacity for CO_2 and a low vapor pressure.

Consequently, we present solubility data of CO_2 and N_2 in different branched and linear polymers. Furthermore, the solubilities of CO_2 in some aqueous polymer solutions are measured because water is also a component of the flue gas (and many other gas streams) and might dissolve in the polymer and decrease the CO_2 solubility. As a modeling approach, we discuss the UNIFAC-FV model.

2. Experimental Methods and Equipment

2.1. Materials. The investigated linear, branched, and dendritic polymers and some characteristic properties are depicted in Table 1. The linear and branched polyethers were synthesized from ethylene oxide and propylene oxide by Degussa (Germany) and provided with different functional groups, namely hydroxyl and methyl functionalities. The hyperbranched polyesters from Perstorp Specialty Chemicals AB (Sweden) belong to the Boltorn family (B-U3000 and B-H2004), which are produced from polyalcohol cores and bis(hydroxymethyl)propionic acid (bis-MPA). The hydroxyl functionalities are partially esterified with medium-length (60%, B-H2004) and long-chain C_{16-18}-fatty acids (90%, B-U3000). The second generation polyamidoamine dendrimer (PAMAM) with hydroxyl functionality was obtained from Dendritech (USA). The core consists of ethylenediamine and is further built up with methyl acrylate followed by amidation of the resulting carbomethoxy intermediate with ethylenediamine.[6] The macromolecule consists of amide and ternary amino groups. The polyethylene imine (Lupasol FG) was a donation from BASF (Germany). Inside the molecule there are various primary, secondary, and tertiary amino groups. Further details are given by Petersen.[12]

Apart from these nonvolatile polymers, degassed deionized water was used; carbon dioxide (purity ≥99.7%) and nitrogen (purity ≥99.999%) were purchased from Linde (Germany).

2.2. Gas Solubility in Polymer Melts and Aqueous Polymer Solutions. In this work, gas solubilities were measured using an apparatus following principles described by Reichl et al.[13,14] We definitely prefer stirred vessels to nonagitated measurements, e.g., in the Rubotherm magnetic suspension balance. Figure 1 shows a schematic flow diagram of the experimental setup that was used in this work. The equilibrium cell (7) is provided with a magnetic stirrer (8) and placed inside an air thermostat (6). The cell temperature is determined with a resistance thermometer (Pt 100) in an immersion sleeve. The cell is connected via a valve and a quick connection to a gas system (3) which contains the solute and is located in another air thermostat (2).

Table 2. Technical Data of the Apparatus

quantity	equipment, company	range of measurement	resolution	precision of measurement
pressure	pressure sensor I, WIKA	0−1.6 bar	0.0001 bar	±0.0016 bar
	pressure sensor II, WIKA	1−10 bar	0.001 bar	±0.010 bar
temperature	resistance thermometer, Conatex	223−673 K	0.01 K	0.1 K
solvent mass	balance, Mettler	0−6100 g	0.01 g	0.1 g
density and temperature	vibration U-tube densimeter, Anton Paar	0−3 g/cm^3	1×10^{-6} g/cm^3	1×10^{-5} g/cm^3
		273−363 K	0.001 K	0.01 K

The gas system contains a pressure sensor. The temperature is measured with a resistance thermometer (Pt 100) inside the thermostat. The gas is fed from a reservoir (1) to the system. The cell and the gas system are attached to a vacuum pump (9). The measured data (temperature in the cell and in the gas system, pressure in the system) are collected from a multimeter (Keithley 2700/E) and recorded with a computer.

In Table 2, technical data of the apparatus and the measured quantities are given. The apparatus was designed for $T_{max} = 373$ K and $P_{max} = 10$ bar. The volume of the cell was measured as 1.182×10^{-4} m^3 ($\pm 10^{-7}$ m^3) by filling the cell with degassed water at a known temperature for several times and weighing the mass of water. The volume of the gas system was calculated by pressure drop observations between the cell and the gas system to be 2.918×10^{-4} m^3 ($\pm 2 \times 10^{-7}$ m^3).

The degassed (liquid) polymer is filled into the equilibrium cell at constant temperature $T_{cell,1}$ and stirred continuously. After evacuating the system and the cell again, the valve between the cell and the system is closed and the gas is fed from the reservoir (1) to the gas system and allowed to equilibrate for 0.5−1 h until pressure $P_{system,1}$ and temperature $T_{system,1}$ are constant. Then, the gas is admitted into the cell and absorbed until equilibrium is reached at constant pressure $P_{system+cell,2}$. Further, the next temperature $T_{cell,2} < T_{cell,1}$ can be specified and again the pressure decreases to $P_{system+cell,3}$ due to absorption into the polymer and a higher solubility at lower temperatures. The time of equilibration of the whole system (system + cell) depends on the viscosity of the solvent, and the solubility and takes 30−120 min.

The reproducibility of the experimental results was ensured by means of at least two independent measurements. For systems with carbon dioxide, the errors for each Henry constant are around 1−2%. The regeneration of the polymers has been carried out under vacuum at $T > 373$ K.

The validation of the apparatus was approved by determining the Henry constants of CO_2 in H_2O as depicted in Figure 2. The gas solubility measurements in aqueous polymer solutions were performed as described above. In advance, VLE experiments were carried out to determine the activity coefficient of water in the polymer solution. As will be pointed out below, the water activity was taken into account for the calculation of the gas solubility in aqueous polymer solutions. Therefore, the experimental setup was changed. The pressure sensor was connected with the equilibrium cell to measure the pressure of a solution of known composition (volume$_{gas\ phase} \ll$ volume$_{liquid\ phase}$). The error of this measurement is estimated as ≤7%.

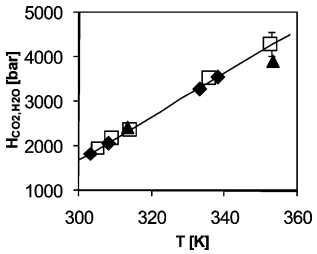

Figure 2. Henry constants of CO_2 in water at different temperatures. Experimental data of (◆) Zheng et al.,[15] (▲) Kiepe et al.,[16] and (□) this work. Solid line: calculated from the equation of Carroll et al.[17]

It is known from recent works[14] that the error of the calculation of the gas-phase concentration increases if the solvent pressure is higher than one-third the system pressure ($P_{system+cell,3}/3$). Therefore, the gas solubility experiments at higher temperature (e.g., $T > 330$ K) were done at a higher total pressure (equilibrium pressure) and with a different pressure sensor (see Table 2). The errors for each Henry constant in the aqueous systems lie from 2 to 5%.

2.3. Density of Polymers and Polymer Solutions. The densities of pure polymers and aqueous polymer solutions were determined with the help of an Anton Paar (Graz, Austria) vibrating U-tube densimeter (DMA 5000). The polymer samples were dried at elevated temperature under vacuum for 2 days until the weight was stable and moisture as well as other volatile components were removed. Several samples from each polymer were investigated. The implemented viscosity correction was chosen for components >500 mPa s. The reproducibility of density for different samples of pure components was in the range from 0.000 06 g/cm^3 (branched and linear polyethers, polyethylene imine) to 0.0005 g/cm^3 (hyperbranched polyester B-U3000) while the observed standard deviation of density for one sample amounts to <0.000 01 g/cm^3. In the beginning of each experimental set, a density check with degassed deionized water was performed to ensure the proper operation of the instrument. Each experimental point was measured independently at least two times to ensure reproducibility. The data given in the tables below are average values for all measurements.

The density of the aqueous polymer solutions was determined similarly. The observed standard deviations of density for different samples of the same concentration differ for the different solutions: 0.000 07 g/cm^3 (Polyether 2); 0.0001 g/cm^3 (Polyether 1, Polyether 3); ≤0.0002 g/cm^3 (PAMAM).

3. Primary Data Reduction and Modeling

3.1. Estimation of Henry Constants. The amount of absorbed gaseous solute can be determined iteratively by *PVT* calculations and solving the material balances.

In case of the binary systems gas−polymer, only the composition of the liquid phase at equilibrium condition (T_{cell}, P_2) is calculated, assuming a negligible vapor pressure of the polymer. The composition of the liquid phase in the measuring cell follows from eq 1, which gives the moles of dissolved gas ($n^L_{gas,cell}$):

$$n^L_{gas,cell} = n^{system}_{gas,1} - n^{system}_{gas,2} - \left(\frac{V^{cell} - \dfrac{m_s + M_{gas} n^L_{gas,cell}}{\rho^L_{mixture}}}{v^G_{gas,cell}} \right) \quad (1)$$

Table 3. Calculated Poynting Corrections ($\Pi_{\infty,i}$) for CO_2 and N_2 at 298.15 K[a]

Carbon Dioxide			Nitrogen		
P [bar]	v_{∞,CO_2} [cm^3/mol]	Π_{∞,CO_2}	P [bar]	v_{∞,N_2} [cm^3/mol]	Π_{∞,N_2}
1.1	55[b]	1.002	1.4	46.5[c]	1.003
4.5	55[b]	1.01	4.5	46.5[c]	1.008
			1.4	65[b]	1.004
			4.5	65[b]	1.012

[a] The pressure was chosen as a mean equilibrium pressure in the experiments for each gas. [b] Handa et al.[17] Estimated value from various systems. [c] Maloney and Prausnitz:[18] fitted function for v_{∞,N_2} in polyethylene ($v_{\infty,N_2} = 16.7 + 0.1T$ [K]).

The difference of moles of gas in the gas system before and after absorption is calculated by means of the Redlich−Kwong−Soave (RKS) equation of state as follows: $n_{gas,1}^{system} = f(T_1,P_1,V_{gas\ system})$ and $n_{gas,2}^{system} = f(T_2,P_2,V_{gas\ system})$. It has been proven experimentally that the density of the mixture $\rho_{mixture}^{L}$ (gas and polymer) in eq 1 does not differ significantly from the density of the pure polymer; the difference (<0.05%) is by far smaller than the assumed error of the density measurement. Therefore, the density of the pure polymer is used. The molar volume of the gaseous phase in the measuring cell ($v_{gas,cell}^{G}(T_{cell},P_2)$) is also obtained from the RKS equation, and the mass of the solvent (m_s) is determined by weighing.

The Henry constant is obtained from the phase equilibrium condition

$$y_i\phi_i P = \Omega_i^* w_i H_{i,j} \exp\left(\frac{v_{\infty,i}(P - P_{SV}^{LV})}{RT}\right) \tag{2}$$

For binary systems, i.e., without water, the gas phase consists of one component only, so the fugacity coefficient of one component in the mixture (ϕ_i) becomes the fugacity coefficient of the pure component ($\phi_{0,i}$). The mass-based activity coefficient (Ω_i^*) in the asymmetric convention is assumed to be unity due to the high dilution.

Test calculations were made to estimate the values of the Poynting correction. Since the liquid molar volumes at infinite dilution of the gases in the solvents are not known, the test calculations were carried out, based on the values estimated according to the data from Handa et al.[18] For CO_2, the Poynting correction has been found to be equal to unity up to the third decimal position and thus can be neglected within the whole range of investigated temperatures and pressures. The same is true for N_2, when the equilibrium pressure is around 1.4 bar at 298 K. At higher pressure (4.5 bar) (chosen for some nitrogen−polymer systems and aqueous systems) the Poynting correction becomes slightly more important, but due to the lack of information on the liquid molar volume of nitrogen at infinite dilution, we decided to neglect it. Table 3 gives some calculation results for the Poynting correction with estimated liquid molar volumes from the literature. If the corresponding Poynting correction is taken into account, the Henry constants of nitrogen increase by 1−1.5%. The error of the measurements is still higher.

For the treatment of ternary systems (aqueous polymer solution as a solvent), the composition of the vapor phase is determined in iteration using the equilibrium condition. The activity coefficient of water refers only to the binary system polymer−water due to the negligible influence of the dissolved gas at high dilution and is obtained by experiment according to eq 3:

$$\Omega_{water} = \frac{P_{water}^{measured}\phi_{0,water}}{w_{water}P_{0,water}^{LV}(T^{measured})} \tag{3}$$

In eq 3, the Poynting correction of the liquid phase was neglected because of the low total pressure (<0.7 bar). If the water concentration in the polymer solution is ≥60 wt %, the system pressure is close to the saturated vapor of water and its activity can be set to unity:

$$a_{H_2O} = P/P_{0,H_2O}^{LV} = w_{H_2O}\Omega_{H_2O} \tag{4}$$

Furthermore, caloric effects such as the enthalpy of absorption at infinite dilution ($\Delta h_{\infty,i}^{LG}$) are calculated. The Henry constant is a measure valid for physical absorption and allows for the calculation of the enthalpy of absorption at infinite dilution. It is accessible from the equilibrium condition combined with the Gibbs−Helmholtz equation and reads as

$$\left(\frac{\partial \ln H_{i,j}}{\partial\left(\frac{1}{T}\right)}\right)_{P,x\to 0} = \frac{\Delta h_{\infty,i}^{GL}}{R} \tag{5}$$

3.2. Modeling Gas Solubility Using UNIFAC-FV. As a modeling approach, we make use of the group-contribution method UNIFAC-FV which has been suggested by Oishi and Prausnitz to model polymer solutions since it is capable of considering differences in the thermal expansion behavior of polymers and solvents, which is of special importance for supercritical components in the mixture.[20] The UNIFAC-FV model allows for the prediction of the solubility behavior if the phase behavior of a system is not known. Therefore, this model can be applied for the design of new polymeric substances with desired CO_2 solubility behavior. According to UNIFAC-FV, the solvent activity results from three contributions (combinatorial a_i^{com}, residual a_i^{res}, and free volume a_i^{FV} parts):

$$\ln(a_i) = \ln(a_i^{com}) + \ln(a_i^{res}) + \ln(a_i^{FV}) \tag{6}$$

Further details on UNIFAC-FV can be found elsewhere.[20−22]

The UNIFAC-FV model was already proven to be of value for the representation of vapor−liquid equilibria of dendritic polymer solutions.[7,22−24] In modeling phase equilibria in systems with dendritic polymers, it is important to take into account the structure and the large number of functional end groups of these polymers. Both peculiarities of the macromolecules show dominating effects on the phase behavior but are not explicitly included in many modeling approaches. Although UNIFAC-FV does not allow for a direct reproduction of the polymer's molecular structure, the impact of structure and functional groups can be indirectly regarded by the different parts of the activity in eq 6.

Seiler et al. focused on the residual part of the activity. In their approach, the calculation of the VLE of dendritic polymer solutions with UNIFAC-FV was related to the observation that only certain kinds of the structural polymer units (linear, dendritic, terminal) dominate the polymer−solvent interactions. Since OH-terminated hyperbranched polymers exhibit comparatively large hydrodynamic radii in good polar solvents, allowing for the penetration of the solvent molecules into the interior of the hyperbranched polymers, it was assumed that all polymeric structure groups (dendritic, linear, and terminal groups) contribute to the residual activity.[22] Tande et al. manipulated the b parameter in the free volume part of the

Table 4. Number of UNIFAC Groups Assignment of the Investigated Polymers

	UNIFAC groups							
polymers	CH_3	CH_2	CH	C	OH	CH_2O	CCOO	CH_2CO
Polyether 2	0	12	1	0	1	10	0	0
Polyether 3	1	14	1	0	0	12	0	0
Polyether 1	17	36	13	4	6	37	0	0
B-U3000	29	185	56	0	2	0	15	14

Table 5. Solubility Data Used for the Fitting of the Interaction Parameters

	systems	number of data points	reference(s)
CO_2−*n*-alkanes	CO_2-C_7, CO_2-C_8, CO_2-C_{10}, CO_2-C_{12}, CO_2-C_{14}, CO_2-C_{16}	34	34
CO_2−*n*-alcohols	CO_2-C_5, CO_2-C_8, CO_2-C_{10}	14	34
CO_2−*n*-ethers	$CO_2-C_4H_{10}O$, $CO_2-C_8H_{18}O$	9	34, 53−55
CO_2−esters	CO_2−ethyl acetate, CO_2−propyl acetate, CO_2−pentyl acetate	12	34

activity with regard to the penetrability of the solvent into the hyperbranched polymer molecule.[23]

Nocon et al. applied the UNIFAC-FV model to calculate gas solubilities in low molecular weight components such as alkanes, alcohols, and ketones.[25,26] They received better results by fitting the missing interaction parameters between the gas component and the UNIFAC structural groups to a sum of all three contributions in eq 6 and not simply to the combinatorial and residual activity as usual. We also make use of this approach.

At first, the polymer structures were analyzed and the functional groups were assigned to UNIFAC structural groups (see Table 4) and CO_2 was defined as a new main group. The information on polymer structure for the polyethers was obtained from the supplier and received via C^{13} NMR. The B-U3000 structure had to be estimated from literature information. Mackay and Carmezini measured the molar mass of the third generation hyperbranched polyester B-H30, and Žagar and Žigon investigated the distribution of linear, dendritic, and terminal groups in the fourth generation molecule B-H40.[27,28] We use the ratio of structure units (linear, dendritic, and terminal units) given by Žagar and Žigon and the molecular mass measured from Mackay and Carmezini for B-H30 and add 14 esterified linoleic acid residues as functional groups on the molecules' surface because the hydroxyl functionality of B-U3000 was esterified with sunflower oil that basically consists of $C_{16,18}$ fatty acids.

Subsequently, the missing interaction parameters were fitted to the literature data on the CO_2 solubility in alkanes, alcohols, ethers, and esters at $P = 1.013$ bar CO_2 partial pressure using the Marquardt method and minimizing the objective function (see Table 5 for information on CO_2 solubility data):

$$F = \frac{1}{\mathrm{ND}} \sum_{i}^{\mathrm{NS}} \sum_{j}^{\mathrm{ND}} \left(\frac{\gamma_{ij,\mathrm{exp}} - \gamma_{ij,\mathrm{calc}}}{\gamma_{ij,\mathrm{exp}}} \right)^2 \tag{7}$$

with ND = number of data points and NS = number of systems; $\gamma_{ij,\mathrm{exp}}$ and $\gamma_{ij,\mathrm{calc}}$ = experimental and calculated activity coefficients (on a mole fraction basis).

The experimental activity coefficients were calculated as follows:

$$\gamma_{\mathrm{CO_2}} = \frac{P_{\mathrm{CO_2}}}{x_{\mathrm{CO_2,exp}} f^0_{\mathrm{CO_2}}} \tag{8}$$

whereas the vapor phase is treated as an ideal one. $f^0_{\mathrm{CO_2}}$ corresponds to the fugacity of the hypothetical pure liquid, since CO_2 is at the supercritical pressure at the system temperature. In the literature several procedures have been established to determine the standard fugacity of this hypothetical liquid. Prausnitz and Shair fitted a universal function for various gases from corresponding states theory, and Nocon et al. computed the hypothetical liquid fugacity by extrapolating a straight line on a plot of $\log f^{\mathrm{S}}_{\mathrm{CO_2}}$ ($= \phi^{\mathrm{S}}_{\mathrm{CO_2}} P^{\mathrm{S}}_{\mathrm{CO_2}}$) vs $1/T$ to supercritical temperatures.[25,26,29] Both ways give similar values for the hypothetical liquid fugacity of CO_2 in the investigated region up to $T = 373$ K. We decided to use the extrapolation. The vapor pressures and the densities of the solvents were calculated by empirical equations given in the DIPPR data bank or by the Yen−Woods estimation method.[30] All other UNIFAC parameters were taken from Poling et al.[31] The molar volume of dissolved CO_2 was calculated according to the Zellner method.[32]

We only focused on modeling the gas solubilities of CO_2 in the polyethers and the polyester, because of the following. The polyamines consist of primary, secondary, and tertiary amino groups. These types of amino groups react with carbon dioxide to form carbamates (and are therefore technically not favored); hence the parameter fitting procedure becomes tedious and time-consuming when many "new" UNIFAC groups occur. Besides, no experimental data are available to calculate missing interaction parameters for the reaction products. In contrast to Nocon et al., we decided to use the standard parameters for b and c constants in the free volume term ($b = 1.28$, $c = 1.1$ instead of $b = 1.4$, $c = 1.0$) to maintain the predictive character of UNIFAC-FV. The r parameter and q parameter (volume and surface parameters representing van der Waals properties) for CO_2 were chosen according to Nocon et al., and are as follows: $r_{\mathrm{CO_2}} = 1.3$ and $q_{\mathrm{CO_2}} = 1.12$. The fitted interaction parameters are given in Table 8.

4. Results and Discussion

4.1. Densities of Polymers and Polymer Solutions. The densities of the solvents are a prerequisite for the calculation of the gas solubility as already mentioned above. In Figure 3, the densities of the pure polymers are plotted in the temperature range from 293.15 K to 363.15 K. The pure polymers' densities decrease with increasing temperature and show a linear trend against temperature. In Figure 4 the densities of the aqueous polyether solutions versus the water concentration are depicted for different temperatures. In the polymer-rich region, the density of the mixture first increases to a maximum around $w_{\mathrm{H_2O}} = 0.15-0.2$ for each temperature. Figure 5 shows the negative excess volumes, obtained from eq 9, for the aqueous solution

$$v^{\mathrm{E}} = \frac{1}{\rho_{\mathrm{mixture}}} - \left(\frac{w_{\mathrm{H_2O}}}{\rho_{\mathrm{H_2O}}} + \frac{w_{\mathrm{polymer}}}{\rho_{\mathrm{polymer}}} \right) \tag{9}$$

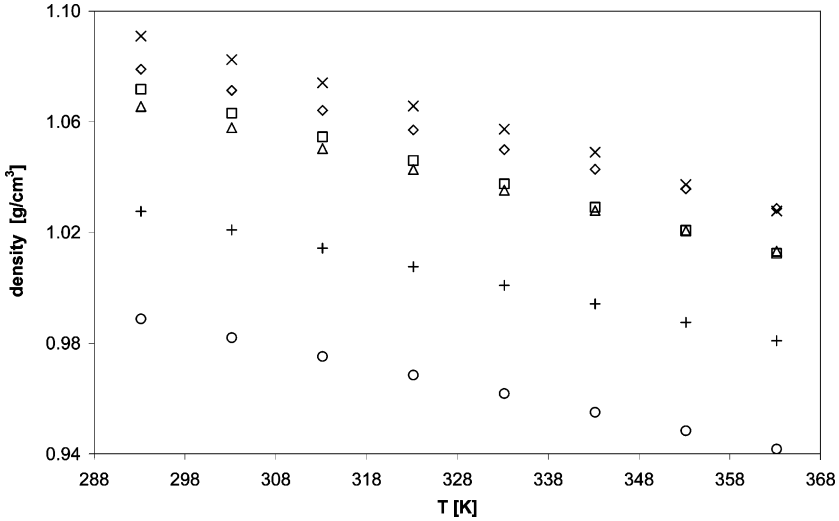

Figure 3. Experimental density data of investigated polymers as a function of temperature: (△) Polyether 1; (×) Polyether 2; (◇) H-2004; (□) Polyether 3; (+) Lupasol FG; (○) B-U3000.

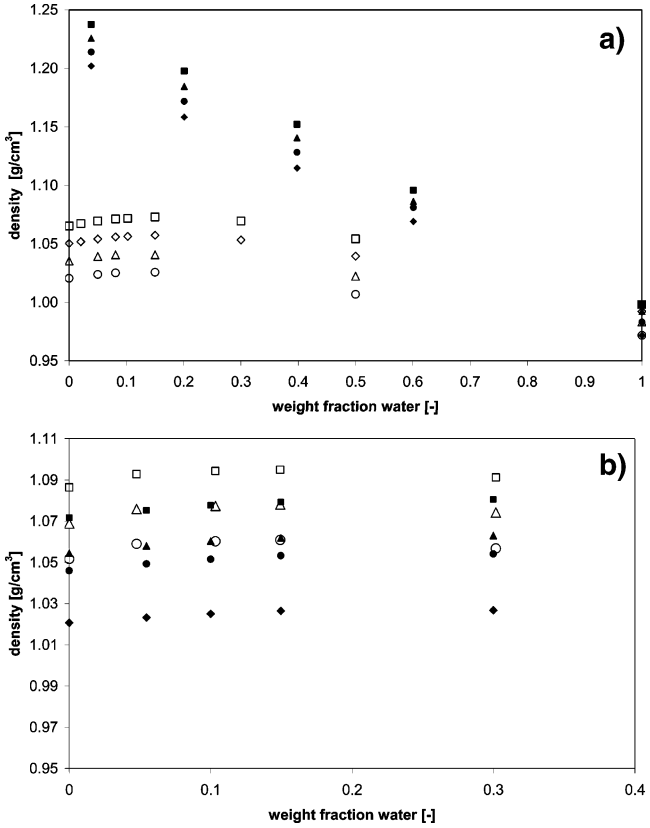

Figure 4. (a) Experimental density data of investigated aqueous branched polymer solutions as a function of temperature: (□) Polyether 1, 293.15 K; (◇) Polyether 1, 313.15 K; (△) Polyether 1, 333.15 K; (○) Polyether 1, 353.15 K; (■) PAMAM, 293.15 K; (▲) PAMAM, 313.15 K; (●) PAMAM, 333.15 K; (◆) PAMAM, 353.15 K. Values for pure water are from Wagner and Pruss.[34] (b) Experimental density data of investigated aqueous linear polyether solutions as a function of temperature: (□) Polyether 2, 293.15 K; (△) Polyether 2, 313.15 K; (○) Polyether 2, 323.15 K; (■) Polyether 3, 293.15 K; (▲) Polyether 3, 313.15 K; (●) Polyether 3, 323.15 K; (◆) Polyether 3, 353.15 K. Values for pure water are from Wagner and Pruss.[34]

of the branched Polyether 1 for different temperatures. Different contributions compete for the excess volume of the asymmetrical and polar mixture, free volume effects, and hydrogen bonding between water molecules and between water and polymer molecules. The resulting impact on the excess volume can be seen in Figure 5. An increase in temperature leads to a decrease in excess volume.

Müller and Rasmussen report a similar behavior for aqueous linear polyethylene glycol solutions, resulting from the polyethylene glycol chain, forming helical structures and grouping up to three water molecules around one ether group that leads to negative excess volumes.[33] At higher temperatures the differences in thermal expansion increase, but the hydrogen bonds are weakened and hence the excess volume decreases.

The plot of the density of the aqueous PAMAM solution versus water concentration for different temperatures (Figure 4a) rather gives a linear interrelationship with temperature over the entire concentration range. In Figure 6, the excess volumes for different temperatures are depicted. The density of the pure polymer was estimated by extrapolation from the curves in Figure 4a. In the polymer-rich region, negative excess volumes are obtained, whereas v^E changes into positive when the solvent concentration is increased. The influence of temperature is negligible.

4.2. Solubility Measurements, Selectivity, and Modeling. Knowing the density of the polymer as a function of temperature, it is possible to treat the data, measured with the gas solubility apparatus and finally determine gas solubilities. In Figure 7, the weight-fraction Henry constants for CO_2 in the systems with different linear, branched, and hyperbranched polymers are plotted versus temperature. All Henry constants show a linear dependence on temperature. The solubility decreases as Polyether 3 > Polyether 2 > Polyether 1 > B-U3000 > B-H2004. The hyperbranched polyesters dissolve less CO_2 than the polyethers. The linear Polyether 3 with a $-CH_3$ end group possesses the highest loading among the polyethers. The modification of the end group (PE2, OH → PE3, CH_3) leads to an increase in CO_2 capacity of 15%. However, considered on a molar basis, there is a linear relation between the molar CO_2 loading and the number of C−O−C links in the molecule as depicted in Figure 8.

Comparing the capacity for CO_2 of the polyethers with industrial solvents, Polyether 3 performs similar to the commercial solvent Selexol, as can be seen in Figure 7. The Selexol process, which utilizes a mixture of homologues of the dimethyl ether of polyethylene glycol as a solvent, is a licensed process of UOP and is realized in more than 20 plants for the bulk removal of CO_2 from various high-pressure gas streams such as synthesis and natural gases.[36,37] Since Polyether 3 is of a

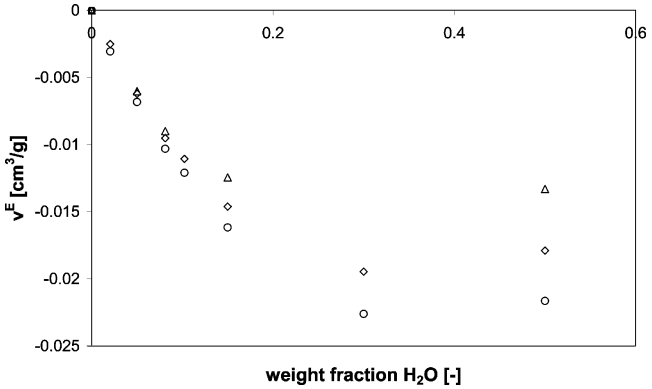

Figure 5. Calculated excess volumes for aqueous polyether (Polyether 1) solution for different temperatures: (△) 333.15, (◇) 313.15, and (○) 293.15 K.

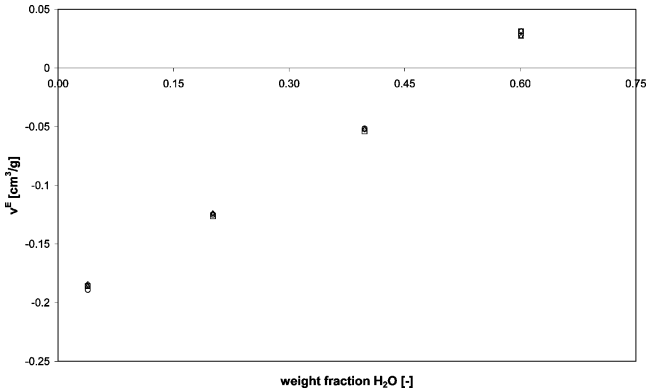

Figure 6. Calculated excess volumes for aqueous PAMAM solution for different temperatures: (□) 293.15, (◇) 313.15, (△) 333.15, and (○) 353.15 K.

molecular structure similar to that of Selexol, the observed solubilities are not surprising. It is obvious that Polyether 3 (as well as Selexol) does not fit as a proper solvent for CO_2 scrubbing from postcombustion flue gas, because the solubility is too low.

Figure 7 also gives the solubility of CO_2 in the ionic liquid (IL) [bmim][Pf6], which has been chosen as a model IL and was discussed for flue gas applications by Anthony et al.[42,43] Compared to the polyethers, the ionic liquid offers similar solubilities, but is sold at a very high price.

Among the polymers that were experimentally investigated, polyethylene imine Lupasol FG has the highest CO_2 solubility

Table 6. Enthalpies of Absorption at Infinite Dilution for CO_2 in Different Polymers, Calculated from Experimental Henry Constants[a]

component	$\Delta h_{\infty,i}^{LG}$ [kJ/mol]
B-H2004	−10.2
B-U3000	−10.4
Polyether 1	−12.1
Polyether 2	−13.3
Polyether 3	−13.5
PAMAM, 61 wt % H_2O	−23.9
MEA, 70 wt % H_2O	−85.0

[a] Value for aqueous 30 wt % MEA solution is taken from Anthony et al.[43]

due to the large number of amino groups (primary, secondary, and tertiary amino groups in the ratio 1:1:1[12]) in the polymer molecule. A temperature increase of 2−4 K accompanies the absorption experiments, indicating a considerable heat of mixing and/or chemical absorption effects. The measured solubilities are high and rather scattered. Obviously, the solubility strongly depends on the regeneration of the polymer after the experiment. Further investigations on the detection of the carbamate group in the CO_2-loaded polymer seem necessary.

As known from the literature, some research groups and companies investigated the benefit of polyamines or hindered amines.[38−41] The amino groups in molecules of this type do not directly react with carbon dioxide like ordinary primary and secondary amino groups, which form rather stable carbamates with CO_2.

The tertiary amino groups of the polymer are unable to form carbamates, whereas the secondary amino groups of the polymer might act as hindered amines, because they are attached to bulky substituents (secondary carbon atoms). The carbamates of hindered amines are of a very low stability (the carbamate stability is 125 times weaker compared to MEA[39]). Sartori and Savage reported that sterically hindered amines offer broader thermodynamic cyclic capacities than MEA and hence lead to a reduction of scrubbing solution and less energy for solvent regeneration.[39] Additionally, Mimura et al. demonstrated that the hindered amines of the KS family feature lower heats of absorption and a broader cyclic capacity, and can be regenerated at a lower temperature; in sum, they are less energy intensive compared to MEA.[41]

Nevertheless, sterically hindered and also tertiary amines often exhibit lower absorption kinetics. There are different possibilities in dealing with this drawback already pointed out in the

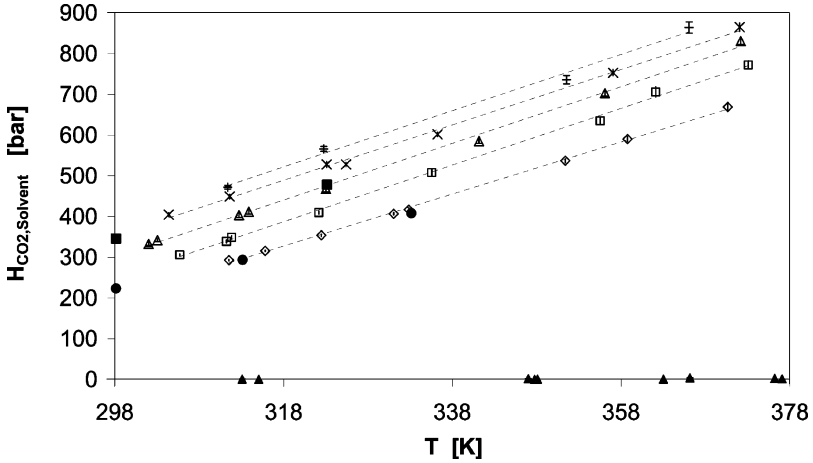

Figure 7. Temperature dependence of weight-fraction-based Henry constants of CO_2 in different polymers, [bmim][Pf6], and Selexol: (+) H-2004; (×) B-U3000; (△) Polyether 1; (□) Polyether 2; (◇) Polyether 3; (▲) Lupasol FG; (●) Selexol from Xu et al.;[36] (■) [bmim][Pf6] from Anthony et al.[38] The dotted lines are given for better visualization.

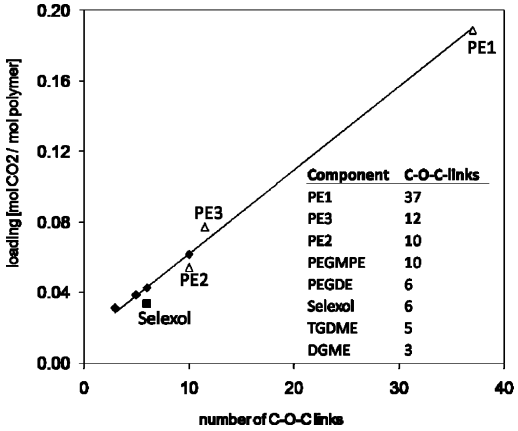

Figure 8. CO_2 loading vs number of C−O−C links in different polyethers. (△) PE1 (Polyether 1), PE2 (Polyether 2), and PE3 (Polyether 3) (this work); (■) Selexol from Xu et al.;[36] (◆) different ethers. Data taken from Fogg et al.[35] The line is given for better visualization.

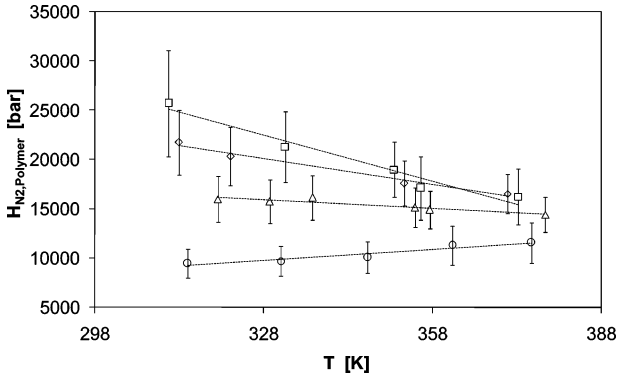

Figure 9. Temperature dependence of weight-fraction-based Henry constants of N_2 in different polymers: (○) B-U3000; (△) Polyether 1; (□) Polyether 2; (◇) Polyether 3; (×) PAMAM, 61 wt % H_2O. The dotted lines are given for better visualization.

literature. It is common to enhance the mass transfer, if necessary, with optimized packings or by adding low concentrations of primary or secondary amines.[37,41] In this work we focus on the thermodynamics and not on absorption kinetics, which must be studied further on.

The plots of the Henry constants allow for the determination of enthalpies of absorption. Table 6 gives the enthalpies of absorption at infinite dilution calculated from eq 5. It can be concluded that the absorption enthalpies of the polyethers and polyesters are much lower in comparison to those of the MEA solution, which represents a chemical absorption. Therefore, physical absorption is presumed, which is preferable for a lower regeneration effort.

Summarizing the absorption behavior of the investigated branched and linear polymers, it is obvious that a very broad solubility range is covered and that a predominantly physical absorption performance is possible. However, an ideal polymeric solvent for CO_2 removal should show low values of the Henry constant at low temperatures (in the region of 313 K), having a very high capacity together with a steeper slope of the Henry curve.

An important requirement for flue gas separations is marked by the demand of the solvent for a high selectivity to separate CO_2 from N_2. Figure 9 gives the solubility of nitrogen in some polymers.

The hyperbranched polyester (B-U3000) and all polyethers have very low N_2 solubilities. The polyethers show only a weak influence of temperature on the solubility over the wide

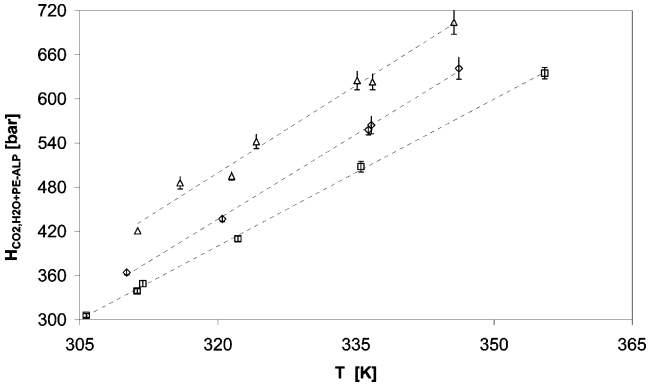

Figure 10. Weight-fraction-based Henry constants of CO_2 in aqueous polyether solutions (Polyether 2) vs temperature: (□) 0 wt % H_2O; (◇) 3.2 wt % H_2O; (△) 6.1 wt % H_2O. The dotted lines are given for better visualization.

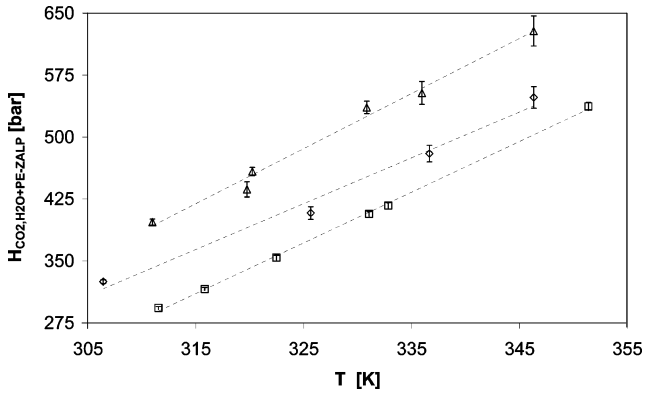

Figure 11. Weight-fraction-based Henry constants of CO_2 in aqueous polyether solutions (Polyether 3) vs temperature: (□) 0 wt % H_2O; (◇) 4.2 wt % H_2O; (△) 9.7 wt % H_2O. The dotted lines are given for better visualization.

temperature range from $T = 310$ to 380 K. Moreover, the solubility increases with increasing temperature. This kind of behavior is known for solutes with a low critical temperature. For such systems, the temperature-dependent solubility runs through a minimum. The location of this minimum and the associated temperature thereof is often found at low temperatures for light gases.[44] It is possible that the nitrogen polymer systems are in the described temperature region.

Knowing the solubilities of CO_2 and N_2, the selectivity of the polymers can be calculated from eq 10, where the partial pressure of the gases in the feed ($P_{N_2} = 0.7$ bar; $P_{CO_2} = 0.12$ bar for a flue gas from a coal-fired power plant) are also taken into account:

$$S_{CO_2,N_2} = \frac{H_{N_2,\text{polymer}} P_{CO_2}^{\text{feed}}}{H_{CO_2,\text{polymer}} P_{N_2}^{\text{feed}}} \tag{10}$$

The polyethers show a high selectivity for CO_2 that is between 7 and 12 (see Table 7); a sharp separation affords for $S = 4$ according to Seider et al.[45]

Figures 10−12 depict the solubility of CO_2 in aqueous polymer solutions for different concentrations. Water is also an important component of flue gas (6−10 mol %) and will dissolve in the polymers to a certain extent. Hence, its influence on the solubility is crucial to know. The polyether−water systems have been investigated only for lower water concentrations. As expected, the CO_2 solubility in both linear polyethers (Figures 10 and 11) decreases with increasing water content,

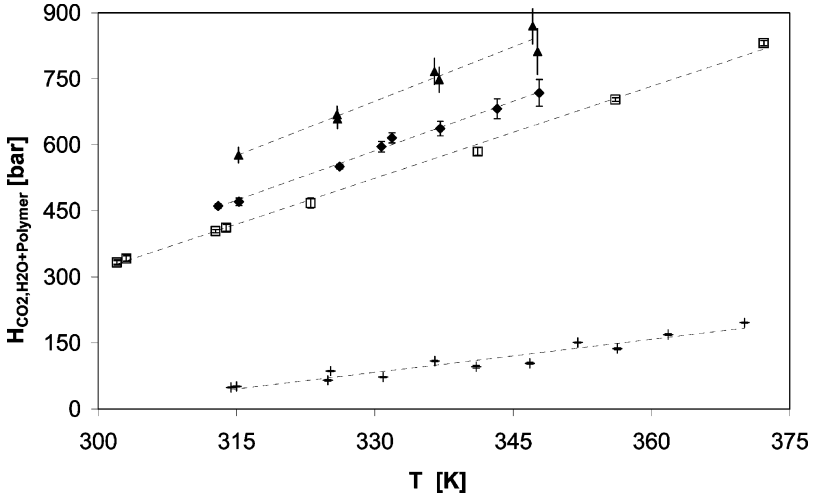

Figure 12. Weight-fraction-based Henry constants of CO_2 in aqueous polymer solutions vs temperature: (□) Polyether 1, 0 wt % H_2O; (◆) Polyether 1, 6.6 wt % H_2O; (▲) Polyether 1, 15.4 wt % H_2O; (+) PAMAM, 61 wt % H_2O. The dotted lines are given for better visualization.

Table 7. Selectivity CO_2/N_2 for Different Polymers at 313.15 K, Calculated According to Eq 5 with Assumed Flue Gas Partial Pressures $P_{N_2} = 0.7$ bar and $P_{CO_2} = 0.12$ bar

polymer	S_{CO_2,N_2}
B-U3000	3
Polyether 1	7
Polyether 2	12
Polyether 3	12
PAMAM, 61 wt % H_2O	81

but still shows a linear behavior of the Henry constant vs temperature. The branched polyether (Figure 12) also exhibits a linear interrelationship with temperature.

The CO_2 solubility in aqueous PAMAM solutions is shown in Figure 12. The pure dendrimer was not considered for solubility measurements because its viscosity is too high for the utilized gas solubility apparatus. The aqueous polyamidoamine dendrimer solution represents also a very good solvent for carbon dioxide, mainly because of numerous tertiary amine groups. Like sterically hindered amino groups, the amide groups are reported not to react directly with CO_2.[46] The tertiary amines react with CO_2 in aqueous solutions and lead to the formation of the bicarbonate ion:[47]

$$CO_2 + R_1R_2R_3N + H_2O \leftrightarrow HCO^{3-} + R_1R_2R_3NH^+ \quad (11)$$

The solubility results are qualitatively confirmed by the work of Kovvali et al. and Duan et al., who already investigated PAMAM dendrimers of generation zero for membrane applications as immobilized liquid membranes and composite membranes for CO_2/N_2 separation.[8,48,49] They received a remarkable permeance and selectivity for CO_2.

The value of the enthalpy of absorption given in Table 6 also indicates that both physical absorption and weak chemical absorption take place. It is considerably lower than the reported values for the heats of absorption for hindered amines (or tertiary amines like TEA and MDEA); the latter is approximately around 10−15% (or 30−40% for tertiary amines) lower compared to MEA.[43,50]

The modeling results are depicted in Figures 13 and 14. The solubility of carbon dioxide in the investigated polyethers and polyesters versus temperature at 1.013 bar is plotted. The UNIFAC-FV model is able to predict the solubility of CO_2 in linear and branched polyethers and the hyperbranched polyester (the fitted interaction parameters are depicted in Table 8). A

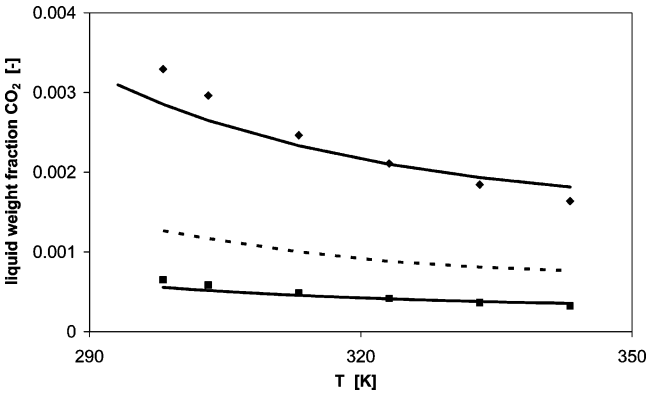

Figure 13. UNIFAC-FV results for solubility of CO_2 in Polyether 1 at different pressures. Experimental solubilities were calculated from Henry constants from Figure 7. (◆) Polyether 1 at 1.013 bar; (■) Polyether 1 at 0.2 bar. Continuous lines, original UNIFAC-FV; dotted line, UNIFAC-FV (Lyngby) for Polyether 1 at 1.013 bar. All calculations are made with $b = 1.28$ and $c = 1.1$.

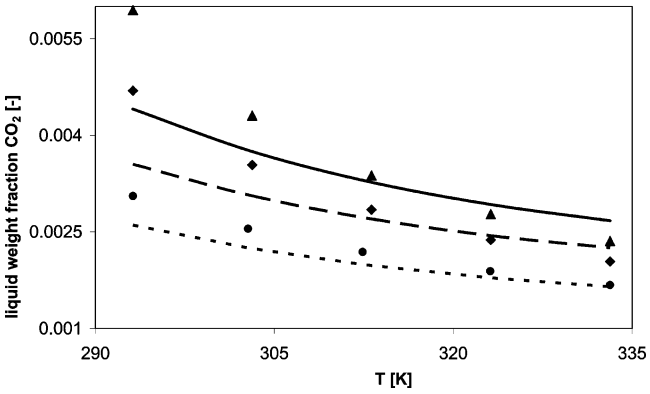

Figure 14. UNIFAC-FV results for solubility of CO_2 in the linear Polyether 2, linear Polyether 3, and the hyperbranched B-U3000 at 1.013 bar. Experimental solubilities were calculated from Henry constants from Figure 7. (▲, —) Polyether 2; (◆, − −) Polyether 3; (●, ···) B-U3000. All curves are results from the original UNIFAC-FV and $b = 1.28$ and $c = 1.1$.

reasonable agreement with the experimental values is reached even at different pressures as shown, for example, for the branched polyether Polyether 1 in Figure 12. Nevertheless, the poor consideration of the temperature dependence of the activity coefficient can be observed in the slope of the UNIFAC-FV curves. Circumvention of this lack in the model by has been tried by use of the modified UNIFAC model (Lyngby) of Larsen et al.[51] In the framework of this modification, the interaction

Table 8. Fitted Interaction Parameters of the Original UNIFAC-FV Model

variable	value
UNIFAC-FV parameters	
a_{CO_2,CH_2}	−305.3
a_{CH_2,CO_2}	893.4
F	0.0029
UNIFAC-FV parameters	
$a_{CO_2,OH}$	5134
a_{OH,CO_2}	305.4
F	0.0077
UNIFAC-FV parameters	
a_{CO_2,CH_2O}	−83.75
a_{CH_2O,CO_2}	443.47
F	0.0026
UNIFAC-FV parameters	
$a_{CO_2,CCOO}$	0.73857
a_{CCOO,CO_2}	32.61
F	0.0020

Table 9. Fitted Interaction Parameters of the UNIFAC-FV (Lyngby) Model

variable	value
UNIFAC-FV parameters (Lyngby)	
$a_{CO_2,CH_2,i}$ [a]	2047.3, −60.32, −385.97
$a_{CH_2,CO_2,i}$	−74.7, −1.3217, −25.805
F	0.00017
UNIFAC-FV parameters (Lyngby)	
$a_{CO_2,OH,i}$	444.9, 8.95, 0.0
$a_{OH,CO_2,i}$	−68.21, 1.317, 0.0
F	0.0029
UNIFAC-FV parameters (Lyngby)	
$a_{CO_2,CH_2O,i}$	310.16, 8.681, 0.0
$a_{CH_2O,CO_2,i}$	−334.59, −1.705, 0.0
F	0.00009

[a] $i = 1, 2, 3$.

parameters are temperature dependent (three pairs of parameters per each pair of groups). The unavailable interaction parameters needed for the CO_2-solubility calculations were fitted as described above and are given in Table 9. The free volume term was taken into account. From Figure 13, it can be concluded that the modified UNIFAC-FV (Lyngby) model (the dotted line for CO_2 solubility at 1.013 bar in the branched polyether Polyether 1) does not improve the description of the temperature dependence. The calculated activities are by far too large due to the residual part of the activity. Similar results were found for the linear polyethers.

5. Conclusions

The experimental results on the solubility of CO_2 and N_2 in different polymers demonstrate the high potential of branched polymers as designable solvents for the absorption of CO_2. The branched polymers investigated in this work cover a broad concentration range of solubility. A modification of the functional end group ($-OH \rightarrow -CH_3$) increases the mass-based CO_2 solubility by 15% at least for the linear polyethers. The polyethers are comparable with conventional commercial solvents such as Selexol and might be promising absorbents for CO_2 bulk removal from high-pressure feeds, but are not favorable for postcombustion flue gas absorption. The polyamines offer very high CO_2 loadings because of the presence of different kinds of amino groups per molecule. The polyethylene imine consists of primary, secondary, and tertiary amino groups, whereas primary and secondary amino groups directly react with CO_2 to form carbamates. Nevertheless, the bulkiness of the branched polyethylene imine molecule could favor the behavior attributed to sterically hindered amines with a much lower linkage of CO_2. The aqueous PAMAM dendrimer solution gives a remarkable solubility of CO_2 and selectivity toward N_2 together with a moderate enthalpy of absorption ranging between chemical and physical absorption behavior. Even though a dendrimer as absorbent would be too costly, a competitive hyperbranched polymer with similar physical properties could be synthesized. Future simulation work will have to prove if a process synthesis with dendritic polymers is economically comparable with the state-of-the-art processes using solvents like MEA. A closer evaluation of capital and operational costs of the resulting processes will also have to follow. Furthermore, additional experimental investigations concerning the compatibility against other trace components of flue gas such as oxygen, sulfur, and nitrogen oxides as well as metal dust are to be performed.

The UNIFAC-FV model is able to predict the solubility of carbon dioxide in the investigated linear and branched polyethers and the hyperbranched polyester with reasonable accuracy. The calculation of the solubility of other gases such as nitrogen and methane is intended to be done as well as the prediction of aqueous systems.

In general, it has been shown that dendritic polymers offer the possibility to tailor the solubility behavior by modifying the functional end groups. Polyamines such as polyamidoamine and to a certain extent also the polyethylene imine Lupasol FG with different kinds of amino groups acting as sterically hindered amines are promising starting points toward finding a better solvent.

Acknowledgment

We gratefully acknowledge Dr. T. Pott (Degussa AG) for the polyether supply. Furthermore, we would like to thank Perstorp and BASF for providing hyperbranched polyesters and hyperbranched polyethylene imines.

Supporting Information Available: Experimental data for all density measurements and also the Henry constants in pure polymers and binary polymer solutions. This material is available free of charge via the Internet at http://pubs.acs.org.

List of Symbols

a = activity
$\boldsymbol{a}$ = binary interaction parameter [K]
b = parameter in UNIFAC-FV, free volume part
c = parameter in UNIFAC-FV, free volume part
f = fugacity [bar]
F = objective function
$\Delta h_{\infty,i}^{GL}$ = absorption enthalpy at infinite dilution of component i [kJ/mol]
H = weight-fraction-based Henry constant [bar]
m = mass [g]
M = molecular mass [g/mol]
n = number of moles [mol]
ND = number of data points
NS = number of systems
P = pressure [bar]
q = surface area parameter
R = universal gas constant [J/mol K]
r = volume parameter
S = selectivity
T = temperature [K]
V = volume [m^3]

v = molar volume [cm^3/mol]
w = weight fraction
x, y = mole fraction

Abbreviations

B-H2004 = hyperbranched polyester
B-U3000 = hyperbranched polyester
DGME = diethylene glycol dimethyl ether
Lupasol FG = polyethylene imine
MEA = monoethanolamine
PAMAM = polyamidoamine dendrimer
PEGDE = polyethylene glycol diethyl ether
PEGMPE = polyethylene glycol methylpropyl ether
RKS = Redlich−Kwong−Soave equation of state
TGDME = tetraethylene glycol dimethyl ether
VLE = vapor−liquid equilibrium

Greek Letters

γ = mole-fraction based activity coefficient
ρ = density [g/cm^3]
Φ = fugacity coefficient
ν = number of like groups in a molecule
ω = volume fraction
Ω = weight-fraction-based activity coefficient
Ω^* = weight-fraction-based activity coefficient in asymmetric convention

Subscripts

i, j = referring to component i or j
SV = solvent
0 = referring to pure component

Superscripts

S = standard state
GL = from gas to liquid state
LV = liquid/vapor at saturation conditions
res = residual
com = combinatorial
FV = free volume

Literature Cited

(1) Seiler, M. Hyperbranched Polymers: Phase behaviour and New Applications in the Field of Chemical Engineering. *Fluid Phase Equilib.* **2006**, *241*, 155.

(2) Seiler, M.; Jork, C.; Kavarnou, A.; Arlt, W.; Hirsch, R. Separation of Azeotropic Mixtures Using Hyperbranched Polymers or Ionic Liquids. *AIChE J.* **2004**, *50* (10), 2439.

(3) Voit, B. Hyperbranched Polymers−All Problems Solved after 15 Years of Research? *J. Polym. Sci., Part A: Polym. Chem.* **2005**, *43*, 2679.

(4) Voit, B. New Deveploments in Hyperbranched Polymers. *J. Polym. Sci., Part A: Polym. Chem.* **2000**, *38*, 2505.

(5) Jikei, M.; Kakimoto, M. Hyperbranched polymers: a promising new class of materials. *Prog. Polym. Sci.* **2001**, *26* (8), 1233.

(6) Frechet, J. M. J.; Tomalia, D. A. *Dendrimers and Other Dendritic Polymers*; John Wiley & Sons Ltd.: West Sussex, U.K., 2001.

(7) Seiler, M. *Phase Behavior and New Application of Hyperbranched Polymers in the Field of Chemical Engineering*; VDI-Fortschritte-Berichte, Reihe 3 Nr. 820; VDI: Düsseldorf, 2004. (ISBN 3-18-382003-X.)

(8) Kovvali, A. S.; Sirkar, K. K. Dendrimer Liquid Membranes: CO_2 Separation from Gas Mixtures. *Ind. Eng. Chem. Res.* **2001**, *40*, 2502.

(9) Schneider, Q. Putting the Carbon Back. *Nature* **2006**, *442*, 620.

(10) Working Group III of the Intergovernmental Panel on Climate Change, IPCC. *Special Report on Carbon Dioxide Capture and Storage*; Metz, B., Davidson, O., de Coninck, H. C., Loos, M., Meyer, L. A., Eds.; Cambridge University Press: Cambridge and New York, 2005.

(11) White, C. M.; Strazisar, B. R.; Granite, E. J.; Hoffman, J. S.; Pennline, H. W. Separation and capture of CO_2. *J. Air Waste Manage. Assoc.* **2003**, *53* (6), 645.

(12) Petersen, H. Structurally modified Polyethylenimines and their interpolyelectrolyte complexes with DNA as non-viral gene delivery systems. Dissertation, University of Marburg, 2002 (http://archiv.ub.uni-marburg.de/diss/z2002/0110/pdf/z2002-0110.pdf).

(13) Maassen, S.; Reichl, A.; Knapp, H. Measurement at High Dilution: Ecological Significance. *Fluid Phase Equilib.* **1993**, *82*, 71.

(14) Reichl, A.; Knapp, H. Löslichkeiten von FCKW in flüssigen Lösungsmitteln. *DKV-Tagungsber.* **1991**, *18* (2), 261.

(15) Zheng, D. Q.; Guo, T. M.; Knapp, H. Experimental and Modeling Studies on the Solubility of CO_2, $CHClF_2$, CHF_3, $C_2H_2F_4$ and $C_2H_4F_2$ in Water and Aqueous NaCl Solutions Under Low-Pressures. *Fluid Phase Equilib.* **1997**, *129*, 197.

(16) Kiepe, J.; Horstmann, S.; Fischer, K.; Gmehling, J. Experimental Determination and Prediction of Gas Solubility Data for CO_2 + H_2O Mixtures Containing NaCl or KCl at Temperatures between 313 and 393 K and Pressures up to 10 MPa. *Ind. Eng. Chem. Res.* **2002**, *41*, 4393.

(17) Carroll, J. J.; Slupsky, J. D.; Mather, A. E. The Solubility of Carbon Dioxide in Water at Low Pressure. *J. Phys. Chem. Ref. Data* **1991**, *20* (6), 1201.

(18) Handa, Y. P.; Benson, G. C. Partial Molar Volumes of Gases Dissolved in Liquids. Part I. Selected Literature Data and some Estimation Techniques. *Fluid Phase Equilib.* **1982**, *8*, 161.

(19) Maloney, D. P.; Prausnitz, J. M. Solubility of Ethylene in Liquid, Low Density Polyethylene at Industrial-Separation Pressures. *Ind. Eng. Chem. Process Des. Dev.* **1976**, *15* (1), 216.

(20) Oishi, T.; Prausnitz, J. M. Estimation of solvent activities in polymer solutions using a group-contribution method. *Ind. Eng. Chem. Process Des. Dev.* **1978**, *17* (3), 333.

(21) Balashova, I. M.; Mokrushina, L. V.; Morachevskii, A. G. Modeling of Liquid-Vapor Equilibria For Solutions Of Polymers. *Theor. Found. Chem. Eng.* **1996**, *30* (4), 328.

(22) Seiler, M.; Rolker, J.; Mokrushina, L. V.; Kautz, H.; Frey, H.; Arlt, W. Vapor-liquid equilibria in dendrimer and hyperbranched polymer solutions: experimental data and modeling using UNIFAC-FV. *Fluid Phase Equilib.* **2004**, *221* (1−2), 83.

(23) Tande, B. M.; Deitcher, R. W., Jr.; Sandler, S. I.; Wagner, N. J. UNIFAC-FV Applied to Dendritic Macromolecules in Solution: Comment on "Vapor-Liquid Equilibria for Dendritic-Polymer Solutions" (Lieu, J. G.; Liu, M.; Frechet, J. M. J.; Prausnitz, J. M. *J. Chem. Eng. Data* **1999**, *44*, 613−620). *J. Chem. Eng. Data* **2002**, *47* (2), 376.

(24) Kouskoumvekaki, I. A.; Giesen, R.; Michelsen, M. L.; Kontogeorgis, G. M. Free-Volume Activity Coefficient Models for Dendrimer Solutions. *Ind. Eng. Chem. Res.* **2002**, *41* (19), 4848.

(25) Nocon, G.; Weidlich, U.; Gmehling, J.; Menke, J.; Onken, U. Prediction of gas solubilities by a modified UNIFAC equation. *Fluid Phase Equilib.* **1983**, *13*, 381.

(26) Nocon, G.; Weidlich, U.; Gmehling, J.; Onken, U. Prediction of gas solubilities by a modified UNIFAC equation. *Ber. Bunsen−Ges. Phys. Chem.* **1983**, *87* (1), 17.

(27) Mackay, M. E.; Carmezini, G. Manipulation of Hyperbranched Polymers' Conformation. *Chem. Mater.* **2002**, *14*, 819.

(28) Žagar, E.; Žigon, M. Characterization of a Commercial Hyperbranched Aliphatic Polyester Based on 2,2-Bis(methylol)propionic Acid. *Macromolecules* **2002**, *35*, 9913−9925.

(29) Prausnitz, J. M.; Shair, F. H. A Thermodynamic Correlation of Gas Solubilities. *AIChE J.* **1961**, *7*, 682.

(30) Daubert, T. E.; Danner, R. P. *Physical and thermodynamic properties of pure chemicals: Data Compilation*; Hemisphere Publishing Corp.: New York, 1985.

(31) Poling, B. E.; Prausnitz, J. M.; O'Connell, J. P. *The Properties of Gases and Liquids*, 5th ed.; McGraw−Hill: New York, 2001.

(32) Zellner, M.; Claitor, L.; Prausnitz, J. M. Prediciton of Vapor-Liquid Equilibria and Enthalpies of Mixtures at Low Temperatures. *Ind. Eng. Chem. Fundam.* **1970**, *9* (4), 549−564.

(33) Müller, E. A.; Rasmussen, P. Densities and Excess Volumes in Aqueous Poly(ethy1ene glycol) Solutions. *J. Chem. Eng. Data* **1991**, *36*, 214.

(34) Wagner, W.; Pruss, A. The IAPWS Formulation 1995 for the Thermodynamic Properties of Ordinary Water Substance for General and Scientific Use. *J. Phys. Chem. Ref. Data* **2002**, *31*, 387.

(35) Fogg, P. G. T. *Carbon Dioxide in Non-aqueous Solvents at Pressures Less Than 200 kPa*; Solubility Data Series 50; Pergamon Press: New York, 1992.

(36) Xu, Y.; Schutte, R. P.; Hepler, L. G. Solubilities of carbon dioxide, hydrogen sulfide and sulfur dioxide in physical solvents. *Can. J. Chem. Eng.* **1992**, *70*, 569.

(37) Kohl, A. L.; Nielsen, R. B. *Gas Purification*, 5th ed.; Gulf Publishing: Houston, 1997.

(38) De Filippis, P.; Giavarini, C.; Maggi, C.; Rinaldi, G.; Silla, R. Modified Polyamines for CO_2 Absorption. Product Preparation and Characterization. *Ind. Eng. Chem. Res.* **2000**, *39*, 1364−1368.

(39) Sartori, G.; Savage, D. W. Sterically Hindered Amines for CO_2 Removal from Gases. *Ind. Eng. Chem. Fundam.* **1983**, *22*, 239.

(40) Chakraborty, A. K.; Astarita, G.; Bischoff, K. B. CO_2 Absorption in Aqueous Solutions of Hindered Amines. *Chem. Eng. Sci.* **1986**, *41* (4), 997.

(41) Mimura, T.; Shimojo, S.; Suda, T.; Iljima, M.; Mitsuoka, S. Research And Development on Energy Saving Technology For Flue Gas Carbon Dioxide Recovery And Steam System in Power Plant. *Energy Convers. Manage.* **1995**, *36* (6−9), 397.

(42) Anthony, J. L.; Anderson, J. L.; Maginn, E. J.; Brennecke, J. F. Anion Effects on Gas Solubilities In Ionic Liquids. *J. Phys. Chem. B* **2005**, *109*, 6366.

(43) Anthony, J. L.; Aki, S. N. V. K.; Maginn, E. J.; Brennecke, J. F. Feasibility of Using Ionic Liquids for Carbon Dioxide Capture. *Int. J. Environ. Technol. Manage.* **2004**, *4*, 105.

(44) Prausnitz, J. M.; Lichtenthaler, R. N.; de Azevedo, E. G. *Molecular Thermodynamics of Fluid Phase Equilibria*; 3rd ed.; Prentice Hall: London, 1999.

(45) Seider, W. D.; Seader, J. D.; Lewin, D. R. *Process Design Principles, Synthesis, Analysis, and Evaluation*; John Wiley & Sons: New York, 1999.

(46) Kovvali, A. S.; Chen, H.; Sirkar, K. K. Dendrimer Membranes: A CO_2-Selective Molecular Gate. *J. Am. Chem. Soc.* **2000**, *122*, 7594.

(47) Versteeg, G. F.; Van Swaaij, W. P. M. On the Kinetics Between CO2 and Alkanolamines Both in Aqueous and Non-Aqueous Solutions—II. Tertiary Amines. *Chem. Eng. Sci.* **1988**, *43* (3), 587.

(48) Kovvali, A. S.; Sirkar, K. K. Carbon Dioxide Separation with Novel Solvents as Liquid Membranes. *Ind. Eng. Chem. Res.* **2002**, *41*, 2287.

(49) Duan, S.; Kouketsu, T.; Kazama, S.; Yamada, K. Development of PAMAM dendrimer composite membranes for CO_2 separation. *J. Membr. Sci.* **2006**, *283*, 2.

(50) Chakma, A. CO_2 Capture Processes—Opportunities for Improved Energy Efficiences. *Energy Convers. Manage.* **1997**, *38*, 51.

(51) Larsen, B. L. Rasmussen, P.; Fredenslund, A. A modified UNIFAC Group-Contribution Model for Prediction of Phase Equilibria and Heats of Mixing. *Ind. Eng. Chem. Res.* **1987**, *26*, 2274.

(52) Kikic, I.; Alessi, P.; Rasmussen, P.; Fredenslund, A. On the Combinatorial Part of the UNIFAC and UNIQUAC Models. *Can. J. Chem. Eng.* **1980**, *58* (2), 253.

(53) Mohamed, R. S.; Holder, G. D. High Pressure Phase Behaviour in Systems Containing CO_2 and Heavier Compounds with Similar Vapor Pressures. *Fluid Phase Equilib.* **1987**, *32*, 295.

(54) Ohgaki, K.; Katayama, T. Isothermal Vapor-Liquid Equilibria for Systems Ethyl Ether Carbon Dioxide and Methyl Acetate-Carbon Dioxide at High Pressures. *J. Chem. Eng. Data* **1975**, *20* (3), 264.

(55) Zhang, N.; Wang, W.; Zheng, X. *Tianranqi Huagong* **1997**, *22* (6), 52.

Received for review December 19, 2006
Revised manuscript received June 18, 2007
Accepted June 29, 2007

IE061637F